SLAC-PUB-642
August 1969
(EXP) and (TH)

HIGH ENERGY INELASTIC e-p SCATTERING AT 6° AND 10°*

E. D. Bloom, D. H. Coward, H. DeStaebler,

J. Drees, G. Miller, L. W. Mo, and R. E. Taylor

Stanford Linear Accelerator Center
Stanford University, Stanford, California 94305

and

M. Breidenbach, J. I. Friedman,

G. C. Hartmann,** and H. W. Kendall

Department of Physics and Laboratory for Nuclear Science†
Massachusetts Institute of Technology, Cambridge, Massachusetts 02139

ABSTRACT

Cross sections for inelastic scattering of electrons from hydrogen were measured for incident energies from 7 to 17 GeV at scattering angles of 6° to 10° covering a range of squared four-momentum transfers up to 7.4 $(\mathrm{GeV}/c)^2$. For low center-of-mass energies of the final hadronic system the cross section shows prominent resonances at low momentum transfer and diminishes markedly at higher momentum transfer. For high excitations the cross section shows only a weak momentum transfer dependence.

(Submitted to Phys. Rev. Letters)

---

*Work supported by the U. S. Atomic Energy Commission.

**Now at Xerox Corp., Rochester, New York.

†Work supported in part through funds provided by the Atomic Energy Commission under Contract No. AT(30-1)2098.

Inelastic electron-proton scattering at high four-momentum transfer and large electron energy loss has been used to investigate the electromagnetic structure and interactions of the proton.[1] We have measured the double differential cross section $d^2\sigma(E,E',\theta)/d\Omega dE'$ for electrons on hydrogen in a new kinematic region made accessible by the Stanford Linear Accelerator. We report measurements made at 6° and 10° for several incident energies E, and for a range of scattered energies E', beginning at elastic scattering and ending at $E' \approx 3$GeV. Only the scattered electron was detected. In this kind of measurement the two inelastic form factors[2] which describe the electromagnetic properties of the proton are functions of the squared four-momentum transfer, q^2, and the mass of the unobserved hadronic final state, W. We have measured several spectra at each angle to allow the calculation of model independent radiative corrections[3] over a wide range of q^2 and W.

We observe the excitation of several nucleon resonances[4-7] whose cross sections fall rapidly with increasing q^2. The region beyond $W \approx 2$ GeV exhibits a suprisingly weak q^2 dependence. This letter describes the experimental procedure and reports cross sections for $W \geq 2$ GeV. Discussion of the results and a detailed description of the resonance region will follow.[8]

The incident energies at $\theta = 10^\circ$ were 17.7, 15.2, 13.5, 11, and 7. GeV, and at $\theta = 6^\circ$ were 16, 13.5, 10 and 7 GeV. For fixed E and θ, along a spectrum of decreasing E', W increases and q^2 decreases. The maximum range of these variables over a single measured spectrum occurred at an incident energy of 17.7 GeV and an angle of 10°, where W varied from one proton mass to 5.2 GeV, and q^2 from 7.4 $(\text{GeV/c})^2$ to 1.6 $(\text{GeV/c})^2$. For each spectrum E' was changed in overlapping steps of 2% from elastic scattering, through the observed resonance region, to $W \approx 2$ GeV. Then steps corresponding to a change in W of 0.5 GeV were made.

The electron beam from the accelerator was momentum analyzed with values of $\Delta p/p$ between $\pm$ 0.1% and $\pm$ 0.25% and then passed through a 7 cm liquid hydrogen target. Two toroid charge monitors measured the integrated beam current with uncertainties of less than 0.5%. Electrons scattered in the target were momentum analyzed by a double focusing magnetic spectrometer[9] capable of momentum analysis to 20 GeV/c. Particles selected by the spectrometer passed through a system of four hodoscopes to determine their trajectories and then into a pion-electron separation system based on the different cascade shower properties of electrons and pions. This system consisted of a one radiation length slab of lead followed by three scintillation counters (dE/dx counters) to detect showers initiated in the lead. The showers were then further developed in a total absorption counter consisting of 16 one radiation length lead slabs alternated with lucite Cerenkov counters. The dE/dx counters increased the pion-electron separation efficiency by about a factor of 20 at lower E', but were not required for values of E' near the elastic peak. The electron detection efficiency decreased with E' and was 88% at 5 GeV. The uncertainty in the electron detection efficiency was $\pm$ 1.5% above E' = 5 GeV and increased to $\pm$ 4% at E' = 3 GeV.

The momentum acceptance of the spectrometer was $\Delta p/p$ = 3.5% with momentum resolution of 0.1%. The angular acceptance was $\Delta \theta$ = 7 mrad with a resolution of 0.3 mrad. The measured solid angle of the instrument was $.6 \times 10^{-4}$ sr with an uncertainty of $\pm$ 2%.

Extensive tests showed that there could be significant reductions in target density due to beam heating. In order to correct for changes in the density a second spectrometer[10] was simultaneously used to measure protons from elastic electron-proton scattering at low momentum transfer. The angle and momentum settings of this spectrometer remained fixed for each spectrum. Usually the

density reductions were less than 4%, with the maximum value being 13%. An uncertainty of ± 1% was assigned to the measured cross sections for this correction.

The main trigger for an event was provided by a logical "or" between the total absorption counter and a coincidence of two scintillation trigger counters placed before and after the hodoscopes. The event information was buffered and written on magnetic tape by a SDS-9300 on-line computer, which also provided preliminary on-line data analysis.

The cross sections were determined from an event by event analysis of the hodoscopes and the electron-pion discrimination counters. Corrections were made for fast electronics and computer dead times, hodoscope counter inefficiencies, multiple tracks, inefficiencies of electron identification, and target density fluctuations. Yields from an empty replica of the experimental target, typically 7%, were subtracted from the full target measurements. Electrons originating from π^o decay and pair production were measured by reversing the spectrometer polarity and measuring positron yields. This correction is important only for small E' and amounted to a maximum of 15%. The error associated with each point arose from counting statistics and uncertainties in electron detection efficiencies, added in quadrature.

The data were analyzed separately at SLAC and MIT and averaged before each group began radiative corrections. The results of the analyses were in excellent agreement. For the results given in Table I, the two analyses differed from their mean by an average value of 0.35% with an r.m.s. deviation of 1.2%.

The radiative correction procedures had two steps. The first was the subtraction of the calculated radiative tail of the elastic peak from each spectrum. Using the measured form factors for elastic electron-proton scattering, the radiative tail can be calculated to lowest order of α without using the peaking

approximation.[11] Contributions from external and internal bremsstrahlung, including multiple photon emission, were calculated by two different methods. The differences among these methods were noticeable only for data with $E > 15$ GeV and $E' < 4$ GeV, and amounted to less than 2% in the corrected cross section. The maximum elastic tail contributions to our data are 26% of the cross section at $E' = 3.8$ GeV in the 16 GeV, 6° spectrum and 21% at $E' = 3$ GeV in the 17.7 GeV, 10° spectrum.

The second step in the radiative correction procedure was a two-dimensional unfolding employing the peaking approximation.[11,12] All data at one angle were used to calculate the corrected cross sections. The computation involved no specific model for the cross section, but extensive interpolation and some extrapolation of the data were necessary. All experimental results having values of E' greater than the lowest value of E (7 GeV) utilized no extrapolated data. A variety of numerical procedures involving different kinematic contours for interpolation and extrapolation have been studied.

The errors of the measured cross sections were propagated through the radiative unfolding procedure. Additional uncertainties resulted from the numerical procedures and the approximations made in the application of the radiative correction theories. From various studies we believe that uncertainties due to interpolation techniques are less than 1%, and uncertainties due to extrapolation procedures (most important at the lowest E spectrum at each angle) are less than 3%. Errors from theoretical approximations are more difficult to assess. They are small near the elastic peak and increase with decreasing E'; furthermore, they increase with increasing θ. We believe that for this data, errors due to theoretical approximations are on the order of 5% or less.

The results of the MIT and SLAC analyses, which involved different radiative correction procedures, differed typically from their mean by less than 1%,

and nowhere by more than one half of a standard deviation. The results have been averaged, and the differences have been included in the estimate of systematic error.

Figure 1 shows the 10 GeV, 6^{o} spectrum. Figure 1a is the spectrum before radiative corrections. The dashed line is the calculated elastic radiative tail contribution to this spectrum. Figure 1b shows this spectrum after complete radiative corrections, and Fig. 1c shows the ratio of the corrected to the measured data. Figure 2 shows three other corrected spectra with progressively increasing ranges of q^2. The q^2 dependence of the inelastic continuum at large W is clearly much weaker than that of the resonances.

Table 1 summarizes our results for $W \geq 2$ GeV. Data for $W \leq 2.3$ GeV are averages over a small number of neighboring data points, and all other data represent averages over the total spectrometer acceptance. The kinematic variables correspond to the central ray of the spectrometer. The errors are one standard deviation based on counting statistics and electron detection efficiency, propagated through the radiative correction programs. Systematic errors are not included in Table I. Estimates of the combined systematic errors are 5% for $E' > 5$ GeV increasing to 10% at $E' \approx 3$ GeV. These data are in general agreement, to within the stated errors, with the preliminary data reported at Vienna.[7]

We are pleased to acknowledge the assistance of R. Cottrell, C. Jordan, J. Litt, and S. Loken. Professors W. K. H. Panofsky, J. Pine, and B. Barish participated in the initial planning of the experiment. We are indebted to E. Taylor and the Spectrometer Facilities Group, and to the Technical Division under R. B. Neal, especially the Research Area and Accelerator Operations Departments. We appreciate the help of Mrs. E. Miller during the analysis.

REFERENCES

1. J. D. Bjorken, in Proceedings of the International School of Physics "Enrico Fermi," Course XLI, (Ed. J. Steinberger, Academic Press, New York and London 1968).

2. For example, the inelastic cross section may be represented in terms of the form factors W_1 and W_2 as:

$$\frac{d^2\sigma}{d\Omega dE'} = \frac{e^4 \cos^2(\theta/2)}{4E^2 \sin^4(\theta/2)} \left[W_2(q^2, W) + 2W_1(q^2, W) \tan^2(\theta/2)\right] .$$

The squared four-momentum transfer is $q^2 = 4EE' \sin^2(\theta/2)$. The mass of the final hadronic state $W = \left[M_p^2 + 2M_p (E-E')-q^2\right]^{1/2}$. E and E' are the incident and scattered electron energies and θ is the scattering angle, all in the laboratory frame. M_p is the proton mass.

For a discussion of the different form factor notations see F. Gilman, Phys. Rev. 167, 1365 (1968).

3. J. D. Bjorken, Ann. Phys. (N. Y.) 24, 201 (1963).

4. A. A. Cone, K. W. Chen, J. R. Dunning, G. Hartwig, N. F. Ramsey, J. K. Walker, and R. Wilson, Phys. Rev. 156, 1490 (1967); erratum, Phys. Rev. 163, 1854 (1967).

5. F. W. Brasse, J. Engler, E. Ganssauge, and M. Schweizer, Nuovo Cimento 55A, 679 (1968).

6. W. Bartel, B. Dudelzak, H. Krehbiel, J. McElroy, U. Meyer-Berkhout, W. Schmidt, V. Walther, and G. Weber, Phys. Letters 28B, 148 (1968).

7. Preliminary results from the present experimental program are given in the report by W. K. H. Panofsky in the Proceedings of the XIVth Internl. Conf. on High Energy Physics, Vienna, Austria (1968). (CERN Scientific Information Service, Geneva, Switzerland, 1968.)

8. See the following paper for a discussion of results. A description of the results obtained in the resonance region will be published.

9. Brief descriptions of the spectrometer and the hodoscopes may be found in W. K. H. Panofsky, Vol. I, Proceedings of the Internl. Symposium on Electron and Photon Interactions at High Energies, Hamburg, Germany, (1965), (Springer-Verlag, Berlin, 1965); and A. M. Boyarski, F. Bulos, W. Busza, R. Diebold, S. D. Ecklund, G. E. Fischer, J. R. Rees, and B. Richter, Phys. Rev. Letters 20, 300 (1968).

10. R. Anderson, D. Gustavson, R. Prepost, and D. Ritson, Nucl. Instr. and Meth. 66, 328 (1968).

11. L. W. Mo, and Y. S. Tsai, Rev. Mod. Phys. 41, 205 (1969).

12. H. W. Kendall and D. Isabelle, Bull. Am. Phys. Soc. 9, 94 (1964).

TABLE CAPTION

1. Measured cross sections for $W \geq 2.0$ GeV after all corrections. The errors are one standard deviation. The systematic error is not included in the table but is estimated at 5% for $E' > 5$ GeV increasing to 10% at $E' \approx 3$ GeV.

FIGURE CAPTIONS

1. The spectrum at $\theta = 6^{o}$, $E = 10$ GeV (a) before and (b) after radiative corrections. In (a), the dashed line is the calculated elastic radiative tail which is subtracted before the two-dimensional unfolding is started. The elastic peak, but not the radiative tail, has been reduced by a factor of 6. In (c), the solid line is the ratio of the radiatively corrected to the uncorrected cross sections shown in (b) and (a). No systematic errors are shown. The radiative corrections increase the random errors.
2. Three representative radiatively corrected spectra at (a) $\theta = 6^{o}$, $E = 7$ GeV; (b) $\theta = 6^{o}$, $E = 16$ GeV; (c) $\theta = 10^{o}$, $E = 17.7$ GeV. The ranges of q^2 covered are: (a) $0.2 \leq q^2 \leq 0.5$ $(GeV/c)^2$; (b) $0.7 \leq q^2 \leq 2.6$ $(GeV/c)^2$; (c) $1.6 \leq q^2 \leq 7.3$ $(GeV/c)^2$. The elastic peaks are not shown.

TABLE I

θ (deg)	E (GeV)	E' (GeV)	q^2 $(GeV/c)^2$	W (GeV)	$d^2\sigma/d\Omega dE'$ $(10^{-31} cm^2/sr\text{-}GeV)$
6.000	7.000	5.130	.393	2.000	21.5 ± .49
		4.586	.352	2.249	15.6 ± .40
		3.750	.287	2.587	9.33 ± .64
		3.250	.249	2.769	7.96 ± .73
	10.005	7.886	.864	1.998	10.7 ± .23
		7.349	.806	2.249	9.24 ± .20
		6.745	.739	2.502	7.01 ± .27
		5.361	.587	3.001	4.97 ± .24
		3.724	.408	3.501	3.54 ± .30
	13.529	11.00	1.630	1.999	4.26 ± .087
		10.48	1.553	2.249	4.10 ± .093
		9.936	1.473	2.480	3.85 ± .056
		8.512	1.262	3.004	2.79 ± .085
		6.906	1.023	3.505	2.09 ± .11
		5.054	.749	4.004	1.85 ± .11
		3.394	.503	4.404	1.59 ± .27
	16.049	13.16	2.314	1.998	2.19 ± .042
		12.64	2.222	2.250	2.21 ± .043
		12.03	2.116	2.510	2.16 ± .042
		10.69	1.880	3.008	1.84 ± .042
		9.109	1.602	3.507	1.59 ± .056
		7.282	1.280	4.006	1.24 ± .066
		5.644	.992	4.406	1.11 ± .074
		3.851	.677	4.805	1.13 ± .17
10.000	7.010	4.802	1.023	2.000	2.82 ± .090
		4.294	.915	2.250	2.34 ± .099
		3.717	.792	2.504	2.05 ± .12
10.000	10.988	7.915	2.643	2.001	5.66 ± .38
		6.879	2.297	2.509	6.17 ± .27
		5.634	1.881	3.008	5.59 ± .30
		4.163	1.390	3.507	5.19 ± .43
		3.000	1.001	3.856	5.38 ± .77
	13.534	9.737	4.004	2.000	1.80 ± .072
		9.270	3.812	2.252	2.20 ± .083
		8.737	3.593	2.508	2.62 ± .10
		7.534	3.098	3.007	3.03 ± .15
		6.113	2.514	3.506	2.93 ± .15
		4.473	1.839	4.005	2.98 ± .25
		3.000	1.234	4.406	3.75 ± .54
	15.201	10.86	5.016	2.002	.876 ± .058
		9.868	4.558	2.516	1.57 ± .060
		8.691	4.014	3.014	1.94 ± .089
		7.300	3.372	3.512	2.08 ± .083
		5.696	2.631	4.011	1.98 ± .094
		4.258	1.967	4.410	2.26 ± .15
		3.700	1.709	4.555	2.17 ± .22
		3.000	1.386	4.732	2.46 ± .28
	17.696	12.46	6.699	2.002	.336 ± .020
		11.50	6.184	2.514	.617 ± .027
		10.36	5.571	3.012	.957 ± .042
		9.015	4.847	3.510	1.19 ± .057
		7.461	4.012	4.009	1.33 ± .073
		6.069	3.263	4.408	1.32 ± .091
		4.544	2.443	4.808	1.50 ± .15
		3.800	2.043	4.991	1.70 ± .21
		3.000	1.613	5.181	1.79 ± .37

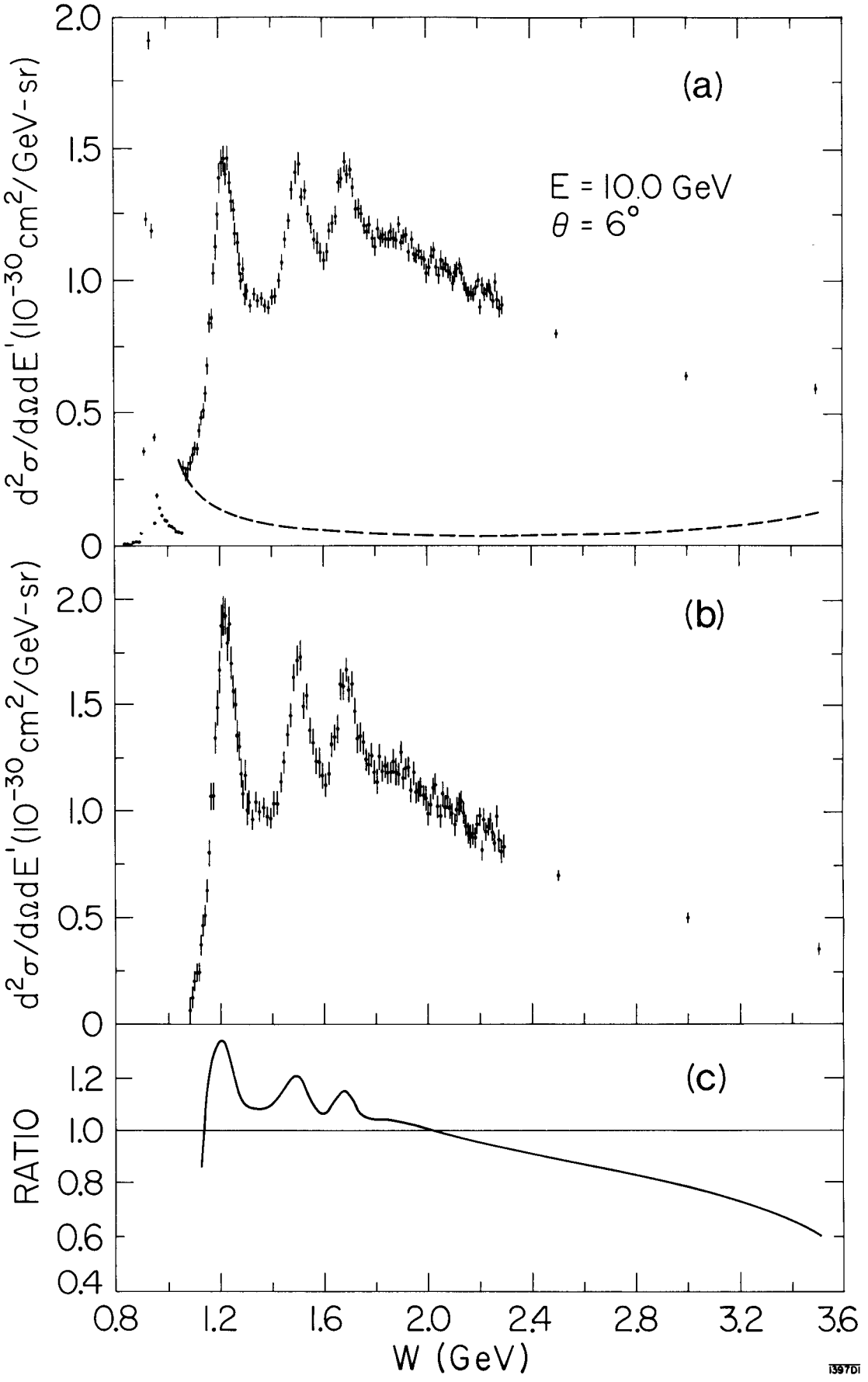

Fig. 1

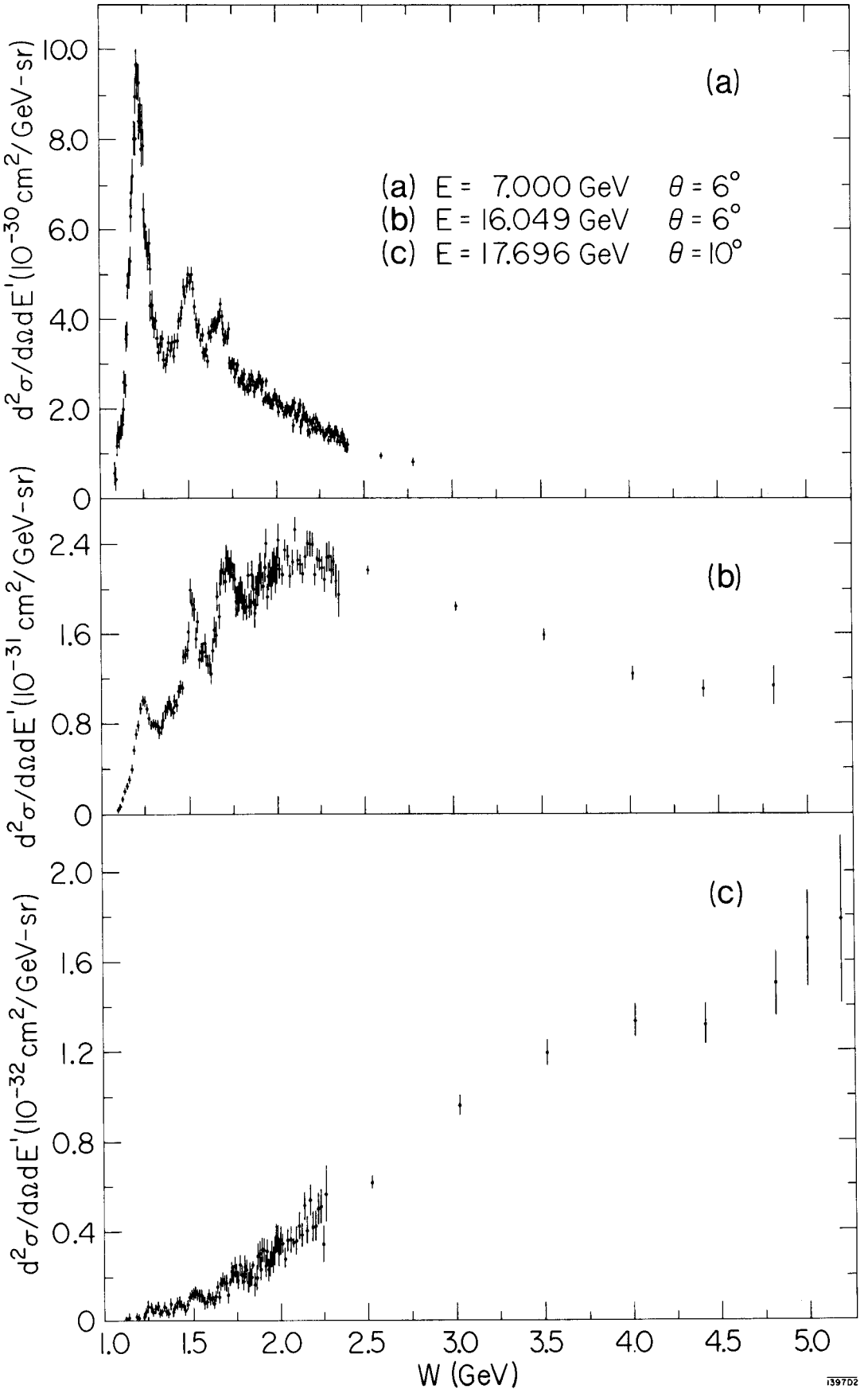
(a)
(a) E = 7.000 GeV θ = 6°
(b) E = 16.049 GeV θ = 6°
(c) E = 17.696 GeV θ = 10°
(b)
(c)
d²σ/dΩdE'(10⁻³⁰ cm²/GeV-sr)
d²σ/dΩdE'(10⁻³¹ cm²/GeV-sr)
d²σ/dΩdE'(10⁻³² cm²/GeV-sr)
W (GeV)
1.0
1.5
2.0
2.5
3.0
3.5
4.0
4.5
5.0
i397D2

Fig. 2